Genetics of Aquatic Organisms 9(1), GA891
https://doi.org/10.4194/GA891

RESEARCH PAPER

Characterization of *TLR6* and *TLR13* Expression in *Litopenaeus vannamei* (Whiteleg Shrimp) During *Vibrio harveyi* Infection

Sunita Subedi[1], Sudarshan Pandey[2], Omkar Vijay Byadgi[2,*]

[1]Department of Tropical Agriculture and International Cooperation, National Pingtung University of Science and Technology, Pingtung, Taiwan.
[2]Aquatic Animal Health Laboratory, International College, International Degree Program of Ornamental Fish Technology and Aquatic Animal Health, National Pingtung University of Science and Technology, Pingtung, Taiwan.

How to Cite

Subedi, S., Pandey, S., Byadgi, O.V. (2025). Characterization of *TLR6* and *TLR13* Expression in *Litopenaeus vannamei* (Whiteleg Shrimp) During *Vibrio harveyi* Infection. *Genetics of Aquatic Organisms, 9(1), GA891*. https://doi.org/10.4194/GA891

Article History
Received 24 February 2025
Accepted 28 April 2025
First Online 30 April 2025

Corresponding Author
E-mail: omkarcof1@gmail.com

Keywords
Aquaculture
Whiteleg shrimp
Vibrio harveyi
Pathogen recognition receptors
Toll-like receptors

Abstract

Litopenaeus vannamei (Whiteleg shrimp) is a crucial crustacean species in global aquaculture, but infectious disease outbreaks, particularly from pathogens like *Vibrio harveyi*, threaten its sustainable growth. Understanding shrimp-pathogen interactions, particularly through Toll-like receptors (TLRs), is essential for improving disease resistance. This study identifies and characterizes TLR6 and TLR13 in Whiteleg shrimp through genome-wide analysis. Using bioinformatics tools, we analyzed their physiological properties, domain structures, multiple sequence alignments, phylogeny, and 3D models. Noticeably, TLR6 and TLR13 contain open reading frames (ORF) encoding 1349 and 1092 amino acids, respectively, with typical leucine-rich repeats, transmembrane, and toll-interleukin-1 receptor (TIR) domains. Multiple sequence alignment indicated the conservation of sequence in the leucine-rich repeat domain. Phylogenetic analysis showed that TLR6 and TLR13 are closely related to *Penaeus japonicus* and *Penaeus monodon*. Quantitative PCR (q-PCR) revealed TLR6 had higher expression in hemocytes and heart, while TLR13 was most expressed in the intestine. After *Vibrio harveyi* infection, TLR6 was upregulated in the gills, though TLR13 showed no significant change in the gills or hepatopancreas. These findings provide new insights into the immune function of whiteleg shrimp's TLR6 and TLR13 against *V. harveyi*.

Introduction

The innate immune system is the primary defense system in crustaceans, which acts as a first line of defense to combat infectious pathogens (Huang & Ren, 2020). Innate immunity relies on the host cells to recognize microorganisms by detecting pathogen-associated molecular patterns (PAMPs). PAMPs include lipopolysaccharide (LPS) from Gram-negative bacteria, double-stranded RNA, single-stranded RNA from viruses, peptidoglycan (PGN), and lipoteichoic acid from Gram-positive bacteria (Wang & Wang, 2013). These PAMPs are recognized by receptors, pattern recognition receptors (PRRs) present in the cells of innate immunity. PRRs are categorized into Toll-like receptors (TLRs), C-type lectin receptors, RIG-I-like receptors, and NOD-like receptors that regulate the process of pathogen recognition and homeostasis between host and microbiota (Habib et al., 2021).

In crustaceans, TLRs have been preserved throughout evolution and play a key role in pathogen recognition (Sánchez-Salgado et al., 2021; Srisuk et al., 2014). TLRs are type I transmembrane proteins having an extracellular domain, a transmembrane, and an intracellular domain (Nie et al., 2018). Several leucine-rich repeats (LRRs) are present at the extracellular N-

terminus, surrounded by N- and C-terminus (LRRNT and LRRCT), respectively. Furthermore, transmembrane domains are present, followed by intracellular Toll/interleukin-1 receptors (TIR) at the C-terminus (Zhou et al., 2015). Additionally, TLRs recognize PAMP ligands through the extracellular LRR domains to initiate signaling cascades, downstream molecules, and, consequently, expression of target genes, including interleukin (IL), type I interferon (IFN), and tumor necrosis factor (TNF) (Habib & Zhang, 2020; Yang et al., 2008).

Whiteleg shrimp (Litopenaeus vannamei) native to the Pacific coast of America, accounts for approximately 85% of the world's total shrimp production (FAO, 2020). It is one of the most popular shrimp species due to its high economic value and relatively short production cycle (Asche et al., 2021). Over the past few years, with the intensification of shrimp culture, high production has been achieved. However, the industry faces various existing constraints caused by pathogens such as viruses, bacteria, and fungi (Jiao et al., 2021). The production of whiteleg shrimp has been especially affected by vibrio species, predominately Vibrio harveyi (Yu et al., 2022).

As a result of advancements in sequencing and data analysis technologies, an increased number of genes for Toll or TLR have been detected in vertebrates and invertebrates that help to investigate their function (Gong et al., 2017; Niu et al., 2023). More than twenty-one TLRs have been identified since the first detection in the mid-1980s (Anderson et al., 1985; Asche et al., 2021). Several functional TLRs have been identified in different species, such as humans, mice, teleost fish, bony fish, and crustaceans. Ten TLRs (TLR1-10) in humans, twelve (TLR1-9 and TLR1-13) in mice, and more than twenty (TLR5, TLR8-20, and TLR22-27) in fish, have been reported. For instance, TLR6 and TLR13 have been studied in both fish and mammals. TLR6 belongs to the TLR1 family and is known to recognize lipoproteins in mice and humans (Gong et al., 2017; Lin et al., 2012; Nie et al., 2018). TLR13 belongs to the TLR11 family and is known to recognize bacterial 23S rRNA in mice whereas they are not present in humans (Gong et al., 2017; Nie et al., 2018; Wang et al., 2016). In addition, TLRs have also been identified in some decapod crustacean species such as crabs and shrimp. However, only (1-9) have been identified in whiteleg shrimp but in our study TLR6 and TLR13 were newly characterized and studied thier expression with V. harveyii infection (Habib et al., 2021; Han et al., 2018; Liang et al., 2018; Wang et al., 2016). The TLRs of fish and mammals share few similarities in their roles in transducing signals. Even though shrimps are not like mammals and fish, shrimps' immune recognition and activation differ from both mammals and fish. The existing literature on the role of novel TLR6 and TLR13 in whiteleg shrimp (L. vannamei) during V. harveyi infection is limited. Understanding their function is crucial for advancing knowledge of the shrimp's innate immune responses. Therefore, this study aims to identify and characterize TLR6 and TLR13 to fill this knowledge gap and support future disease management strategies in shrimp aquaculture.

Materials and Methods

Identification and Characterization of TLR6 and TLR13 in Whiteleg Shrimp

Retrieval of TLR6 and TLR13 in Whiteleg Shrimp

To identify TLR6 and TLR13 in L. vannamei, the data were retrieved from the National Centre for Biotechnological Information (NCBI), Genome Data Viewer database. For further analysis, the nucleotide sequences (Accession Number XM_027373660.1) and (Accession Number XM_027358084.1) were obtained from the NCBI database (https://www.ncbi.nlm-.nih.gov/) in FASTA format.

Sequence Analysis of Whiteleg TLR6 and TLR13

Protein analysis and translation were conducted by ExPASy proteomic tool (https://www.expasy.org/) (Artimo et al., 2012). The physiochemical properties such as molecular weight (MW), theoretical point (pI) and open reading frame (ORF) were computed using ProtParam in ExPASy tool (https://web.expasy.org/-protparam/) (Gong et al., 2017; Han et al., 2018). The protein domain structure was predicted using the Simple Modular Architecture Research Tool (SMART) program (http://smart.embl-heidelberg.de/) (Letunic et al., 2006). Domain structure of TLR6 and TLR13 were compared with other known TLR6 and TLR13 respectively, from vertebrates. Domain structure of TLR6 was compared with human (*Homo sapiens*), mouse (*Mus musculus*), brown rat (*Rattus norvegicus*), domestic cattle (*Bos taurus*), horse (*Equus caballus*), and chimpanzee (*Pan troglodytes*). Concurrently, domain structure of TLR13 was compared with human (*Homo sapiens*), mouse (*Mus musculus*), brown rat (*Rattus norvegicus*), atlantic salmon (*Salmo salar*), dabry's sturgeon (*Acipenser dabryanus*), orange-spotted grouper (*Epinephelus coioides*), and Miu (*Miichthys miiuy*). N-glycosylation sites were predicted using NetNGlyc server (https://services.healthtech.dtu.dk/-services/NetNGlyc-1.0/) (Gupta & Brunak, 2001).

Multiple Sequence Alignment

Multiple sequence alignment of TLR6 and TLR13 was generated using the Clustal Omega in multiple alignment program (https://www.ebi.ac.uk/Tools-/msa/clustalo/) (Qin et al., 2018). Multiple sequence alignments were constructed based on the amino acid sequences of TLR6 and TLR13 with other known TLR6 and TLR13 from vertebrates, including human (*Homo sapiens*), mouse (*Mus musculus*), orange-spotted grouper (*Epinephelus coioides*).

Phylogenetic Analysis

To construct phylogenetic tree, neighbor-joining method was assessed using Molecular Evolution Genetics Analysis (MEGA) software (https://www.mega-software.net/) (Tamura et al., 2021). A bootstrap test with 1000 replications was assessed to verify the reliability of the tree obtained. Protein sequences of other known vertebrates were retrieved from the NCBI database. A phylogenetic tree was constructed to display the phylogenetic relationship between seven representative vertebrate species including, *Penaeus japonicus* (Kuruma prawn), *Trichogramma pretiosum* (Parasitic wasp), *Larimichthys crocea* (Large yellow croaker), *Nasonia vitripennis* (Small parasitoid wasp), *Clupea harengus* (Atlantic herring), *Homo sapiens* (Human), *Mus musculus* (Mouse).

TLR13 was compared with *Eurytemora affinis* (Calanoid copepod), *Girardinichthys multiradiatus* (Darkedged splitfin), *Stegodyphus dumicola* (African social spider), *Armadillidium vulgare* (Pillbug), Nymphon (Sea spiders), *Portunus trituberculatus* (Horse crab), *Eriocheir sinensis* (Chinese mitten crab), *Stegastes partitus* (Bicolor Damselfish), *Nibea albiflora* (Yellow drum), *Homarus americanus* (American lobster), *Cryptotermes secundus* (Drywood termite), *Penaeus monodon* (Giant tiger prawn), *Procambarus clarkia* (Red swamp crayfish), *Lingula anatine* (Common oriental lamp shell), *Hyalella azteca* (Amphipod crustacean), *Xiphophorus helleri* (Green swordtail), *Xiphophorus couchianus* (Monterrey platyfish), *Rhincodon typus* (Whale shark), *Cyclina sinensis* (Blood clam), *Octopus vulgaris* (Common octopus), *Mus musculus* (Mouse), *Penaeus japonicus* (Kuruma prawn).

Secondary Structure Prediction

The secondary structure of the protein was predicted by PSIPRED server (http://bioinf.cs.ucl.-ac.uk/psipred/) (McGuffin et al., 2000).

Three-dimensional (3D) Modeling

The three-dimensional (3D) structure of TLR6 protein was predicted using the Phyre2 server (http://www.sbg.bio.ic.ac.uk/~phyre2/html/page.cgi?id=index).

Gene Expression Analysis of TLR6 and TLR13 in Whiteleg Shrimp

2Experimental shrimp

White leg shrimp (*L. vannamei*), about 1.9 g body weight, were purchased from a local shrimp farm in Pingtung County, Taiwan. Selected shrimp (n=50 shrimp/tank) were kept in a tank containing 400 L of seawater (27 ppt) equipped with a recirculation system for 7 days until no shrimp died. Commercial feed was administered thrice daily, equivalent to 4% body weight. In addition, water replacement was carried out as much as 20% of the total tank volume per day to maintain water quality.

Bacterial Culture and *Vibrio harveyi* Challenge

Vibrio harveyi was kindly provided by Aqua Molecular Genetics Laboratory, Department of Tropical Agriculture and International Cooperation, NPUST. Then, it was cultured in Zobell marine broth (HiMedia, India) for 24 h at 37°C. A challenge test was carried out as described previously by Purbiantoro et al. (2024). Infection was induced by injecting 100 µl phosphate-buffered saline (PBS) containing 106 CFU/shrimp. Thirty shrimps were selected from acclimatized tanks. To prepare for infection, the shrimps were not fed for 24 h. The shrimps were then randomly divided into two groups: treatment and control. The treatment group received an intramuscular injection of 100 µl in the third abdominal segment with 106 CFU/shrimp. In contrast, the control group was injected with a similar amount of phosphate-buffered saline (PBS) only, pH 7.2. Three shrimp from each group were randomly selected at 1-, 2-, and 3-day post-infection (dpi) for tissue sampling post infection.

Sample Collection

Eight samples from healthy tissues were collected including total hemocytes (TH), Intestine (In), Hepatopancrease, Lymphoid organ (LO), Gill (Gi), Heart (He), Muscle (Mu), Eye stalk (Es) for TLR6. The hemolymph was collected using 1.0 mL syringes containing an equal volume of ice-cold anticoagulant (27 mM trisodium citrate; 385 mM sodium chloride, 115 mM glucose, 10 mM HEPES, and pH 7.0). Seven samples for TLR13 were collected from healthy tissues excluding total hemocytes. To evaluate the expression in infected shrimp, gills and hepatopancreases were selected. All samples collected were immediately submerged into 1 mL RNA laterTM solution (Invitrogen by Thermo Fisher Scientific) and maintained at -80°C until RNA extraction.

RNA Extraction and cDNA Synthesis

Total RNA was extracted individually from each shrimp. TRIzol™ Reagent (Invitrogen by Thermo Fisher Scientific, USA) was used for extracting total RNA, following the manufacturer's protocol. The quality and quantity of total RNA were checked by 2% agarose gel electrophoresis (Bio-Rad Laboratories, USA) and spectrophotometry (Eppendorf, Germany). The RNA with the absorbance ratio (A260/280) ranging from 1.8 to 2.0 was used for real-time polymerase chain reaction (RT-PCR) and q-PCR analysis. Total RNA samples of all the experimental groups were reverse transcribed into cDNA using iScript™ cDNA Synthesis Kit (Bio-Rad Laboratories, USA), following the manufacturer's protocol.

Real-time Polymerase Chain Reaction (RT-PCR) Analysis

Real-time PCR was conducted for the amplification of TLR6 and TLR13 in healthy tissues of L. vannamei. cDNA synthesized from the extracted RNA samples was used as the template. The RT-PCR was performed using Labnet Multigene Gradient PCR (Labnet International, USA). The RT-PCR amplifications were performed in a final volume of 25 µl containing Pro Taq 10X buffer, Pro Taq Plus DNA Polymerase, dNTPs with dUTP, MgCl2 (Protech Technology Enterprise, Taiwan), 0.4 µM of each primer, 2.5 µl of DNA template, and sterile water. Specific primers of L. vannamei were designed using NCBI primer blast and Primer3Plus listed in Table 1. The β-actin gene and housekeeping gene were used as an internal control. The qPCR cycling conditions included an initial denaturation step at 95°C for 5 min, followed by 35 cycles of denaturation at 94°C for 1 min, annealing at 58°C for 1 min, and extension at 72°C for 1 min 30 sec, and final extension at 72°C for 10 min. Negative controls included PCR reactions without DNA and RT-PCR without enzyme in the PCR experiments.

Quantitative PCR (qPCR) Analysis

To determine the expression pattern of TLR6 and TLR13 on healthy tissues and after V. harveyi infection in L. vannamei, q-PCR analysis was conducted. Samples were collected from gill and hepatopancreas for TLR13 meanwhile, gill was selected for TLR6. Q-PCR was performed in a 96-well plate and carried out in Connect™ Real-Time System (Bio-Rad Laboratories, USA). Specific primers of L. vannamei were designed using NCBI primer blast and Primer3Plus supplementary table 1. The β-actin gene and housekeeping gene were used as internal control. The q-PCR cycling conditions included preheating at 95°C at 3 min, followed by 40 cycles of denaturation at 95°C at 10 sec, and annealing at 60°C at 30 sec. The comparative CT method ($2^{-\Delta\Delta CT}$) was used to analyze the expression level of the target gene (Livak & Schmittgen, 2001).

Statistical Analysis

The data analysis was performed by using Microsoft Excel (Microsoft Corp., Redmond, and W.A., USA). Analysis of variance (ANOVA) was performed to analyze and calculate the statistical significance for gene expression (IBM SPSS statistics (IBM Corp., Armonk, NY, USA). Different letters indicate statistically significant differences at $P<0.05$ respectively. All data were expressed as mean±standard deviation values. All the graphs were constructed using Origin lab (Origin lab, version 2018; www.originlab.com).

Results

Identification and Characterization of TLR6 and TLR13

Using the Whiteleg genomic resource, TLR6 and TLR13 in L. vannamei were identified. The complete nucleotide sequence of TLR6 and TLR13 comprised 4618 and 4350 bp in length, respectively. TLR6 and TLR13 contained an open reading frame (ORF), which encoded a protein of 1349 and 1092 amino acids, respectively. The calculated theoretical point (pI) of TLR6 and TLR13 were 5.47 and 5.9, respectively. The molecular weight (MW) of TLR6 and TLR13 were 151.7 (kDa) and 123.4 (kDa), respectively. Twelve and thirteen potential N-glycosylation sites were found in TLR6 and TLR13 (Supplementary Figure 1A and 1B).

Domain Structure and Comparison of TLR6 and TLR13

Prediction of protein domains by the SMART program revealed that TLR6 and TLR13 exhibit a typical TLR structure (Figures 1A and 1B). TLR6 contained a signal peptide, 18 leucine-rich repeat (LRR), 5 LRR-TYP domain, an LRR-NT, a transmembrane region (TM), and a Toll/interleukin-I receptor (TIR) domain (Figure 1A). TLR6 domain structure was compared with other known TLR6 from different species; it showed different domain organizations (Figure 2). TLR13 contained a signal peptide, a low complexity region, 10 LRR domain, 2 LRR-TYP domain, an LRR-NT, a TM region and a TIR domain

Table 1. Primers used for gene expression analysis in this study

Primers	Primers sequence 5'-3'	Size	Target	Application
β-actin(F)	*agcacggcatcgtcaccaactg*	129bp	*β-actin*	*RT-PCR*
β-actin(R)	*tagccttggggttgaggggag*			
LvTLR6(F)	*gacgttaccctcggcatcaa*	182bp	*TLR6*	
LvTLR6(R)	*cacgaagttctcgcaggagt*			
LvTLR13(F)	*ggtcggagacaacgagacag*	190bp	*TLR13*	
LvTLR13(R)	*taggacaagggcgatccgta*			
LvTLR6(F)	*gacgttaccctcggcatcaa*	179bp	*TLR6*	*q-PCR*
LvTLR6(R)	*cacgaagttctcgcaggagt*			
β-actin(F)	*ggttgagccctcggatacta*	173bp	*β-actin*	
β-actin(R)	*gagacgcagaaccaagtg*			
LvTLR13(F)	*ggatggggtggttacatttc*	150bp	*TLR13*	
LvTLR13(R)	*gaacaccagggcagtgagtc*			

(Figure 1B). Furthermore, TLR13 also showed different domain organizations when compared to other TLR13s from different species (Figure 3).

Multiple Sequence Alignment of TLR6 and TLR13

The multiple sequence alignment of TLR6 with Homo sapiens (Human) and Mus musculus (Mouse) showed one conserved region in LRR domain (Supplementary Figure 2). Further, multiple sequence alignment of TLR13 with Miichthys miiuy (Miu), Rattus norvegicus (Brown rat), and Epinephelus coloides (Orange-spotted grouper) showed three conserved regions in the LRR domain (Supplementary Figure 3).

Phylogenetic Analysis of TLR6 and TLR13

Phylogenetic trees were constructed with different species to address the evolutionary relationship of TLR6 and TLR13, respectively. The deduced amino acid sequences of TLR6 from 7 species were used for phylogenetic analysis of TLR6. The result revealed that the TLR6 has 100% similarity with Penaeus japonicus (Figure 4). The deduced amino acid sequences of TLR13 from twenty-two species were used for phylogenetic analysis of TLR13. TLR13 has shown 99% similarity with Penaeus japonicus and 72% similarity with Penaeus monodon (Figure 5). Meanwhile, mouse and human TLR6 and TLR13 formed a separate cluster and were only distantly related to TLR6 and TLR13, respectively.

Three-dimensional (3D) Modeling of TLR6 and TLR13

The 3D structure of Whiteleg TLR6 and TLR13 possessed a bending solenoid-like structure. The solenoid structure contained concave and convex regions. The concave region was formed by numerous parallel β-sheet formed due to β-strands. In addition, the convex region was found to be formed by numerous α-helices (Figure 6A and 6B).

Expression of TLR6 and TLR13 in Healthy Tissues by RT-PCR

The mRNA expression of TLR6 and TLR13 in tissues were anlayzed by RT-PCR. The tissues included total hemocytes (TH), Intestine (In), Hepatopancreas, Lymphoid organ (LO), Gill (Gi), Heart (He), Muscle (Mu), and Eyestalk (Es). The results revealed detectable expression levels in all examined healthy tissues in TLR6 (Supplementay Figure 4). Similarly, the results of TLR13 revealed detectable expression in all examined healthy tissues (Supplementary Figure 5).

Expression of TLR6 and TLR13 in Healthy Tissues by q- PCR

The mRNA expressions of TLR6 and TLR13 in tissues were quantified using q-PCR. TLR6 and TLR13 both showed widespread expression, but variable expression was observed in all tested tissues. In TLR6, the expression level was significantly higher in the heart and total hemocyte ($P<0.05$) as compared to other examined tissues. In addition, the intermediate expression level was detected in lymphoid organs followed by the intestine, hepatopancreas and eye stalk, and low levels of expression were detected in muscle and gill (Figure 7A). In TLR13, the expression level was significantly high in the intestine ($P<0.05$) as compared to other examined tissues. Furthermore, the expression level was intermediate in hepatopancreas and muscle. A low level of expression was observed in the lymphoid organ, gill, heart and eye stalk (Figure 7B).

Expression of Whiteleg TLR6 and TLR13 after *V. harveyi* infection by q-PCR

The mRNA level in tissues was quantified using q-PCR to determine the expression patterns in TLR6 and TLR13 in Litopenaeus vannamei after Vibrio harveyi infection (Figure 8A). The relative expression levels of

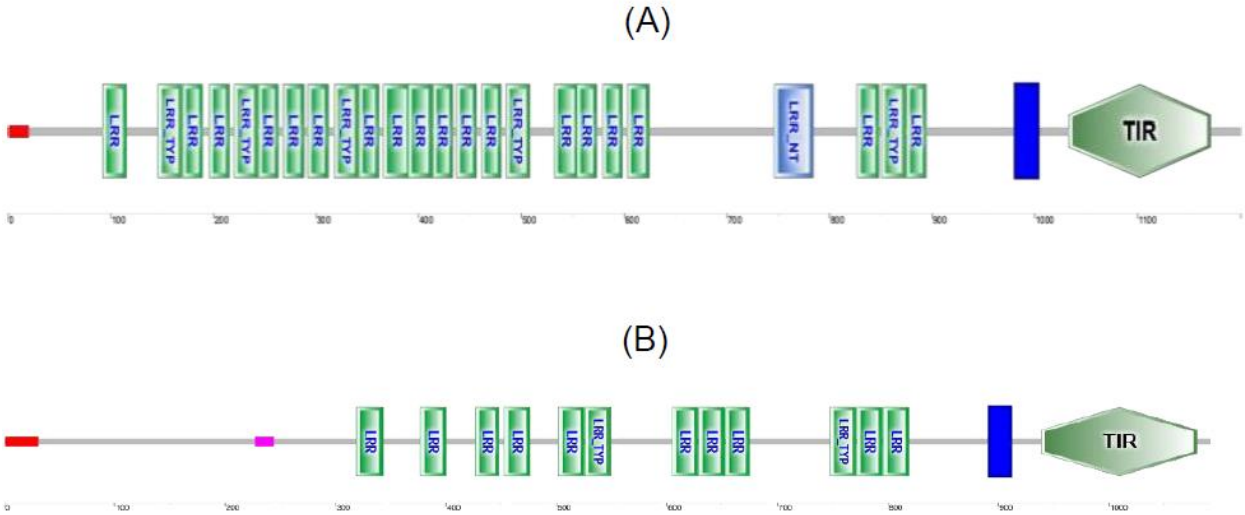

Figure 1. Schematic representation of TLR6 (A) and TLR13(B) domain structure of *Litopenaeus vannamei* (Whiteleg shrimp).

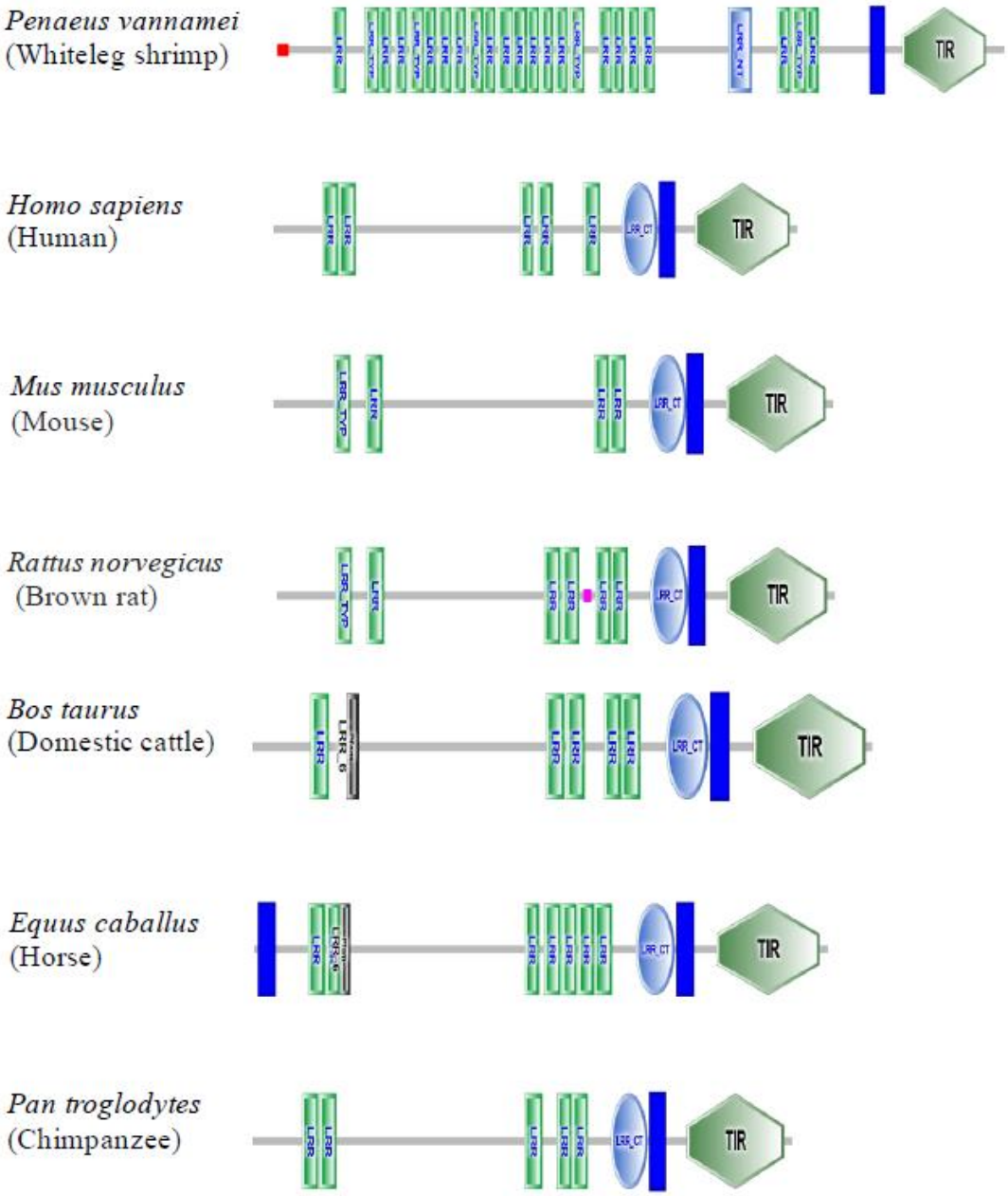

Figure 2. Comparison of domain structure of TLR6 amino acid sequence of *Litopenaeus vannamei* (Whiteleg shrimp) with different species predicted by SMART analysis.

TLR6 were investigated in gill, revealing variable expression patterns over time in response to bacterial infection. In comparison to the control group, Vibrio harveyi infection showed a significant increase ($P<0.05$) in the gill. At 24 hours post-challenge, TLR6 was about 1.25-fold higher. The expression exhibited a gradual decline at 48h to about 1.0-fold. Furthermore, TLR6 expression was increased with the highest level at 72h about 5.2-fold.

Similarly, the relative expression levels of TLR13 in the gills, challenged with Vibrio harveyi were detected at 24-, 48-, and 72-hour post-infection (Figure 8B). The result indicated that TLR6 showed variable expression over time in response to bacterial infection. TLR13 expression levels were lower in the infected group compared to the control group. At 24 hours post-challenge, TLR13 was induced about 1.0-fold and exhibited a gradual decline at 48h to 0.5-fold. However, TLR13 expression was increased with the highest level at 72h with 1.5-fold expression. Furthermore, the relative expression levels of TLR13, challenged with Vibrio harveyi were investigated in the hepatopancreas. TLR13 had variable expression in hepatopancreas over time in response to bacterial infection. Compared to the control group, TLR13 expression levels revealed no significant difference. At 24 hours post-challenge, TLR13 was induced about 1.0-fold expression. The expression exhibited a gradual increase at 48h to 1.2-fold. However, TLR13 expression gradually declined at 72h about 1.0-fold (Figure 8C).

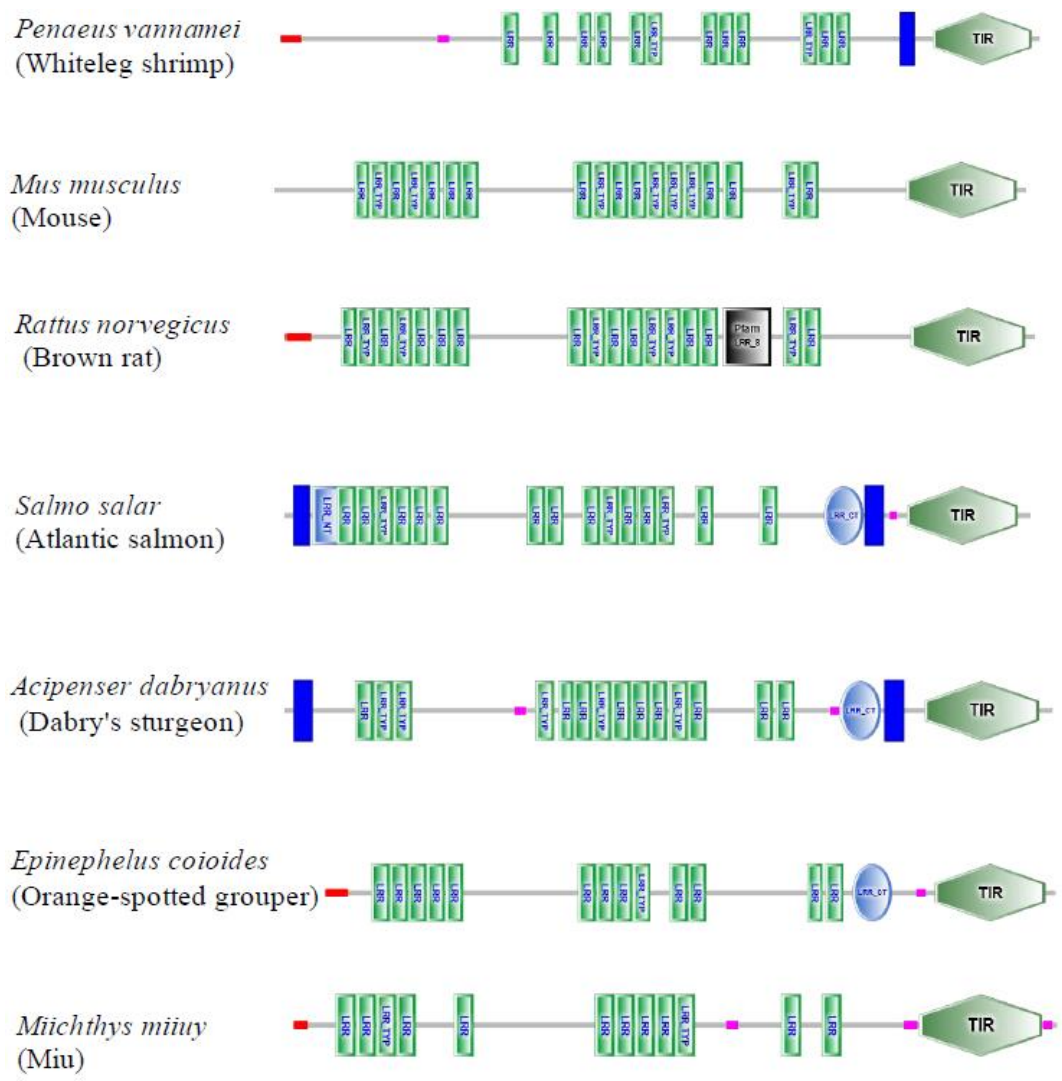

Figure 3. Comparison of domain structure of TLR13 amino acid sequence of *Litopenaeus vannamei* (Whiteleg shrimp) with different species predicted by SMART analysis.

Discussion

Characterization of Whiteleg Shrimp TLR6 and TLR13

TLRs are PRRs that mediate the recognition of PAMPs and play an important role in innate immunity. TLRs are the earliest and most widely studied PRRs in both vertebrates and invertebrates (Qin et al., 2018). In the absence of an in-vivo experiment, bioinformatic analyses were conducted including the molecular mass, theoretical point (pI), potential N-glycosylation sites, domain prediction, phylogenetic analysis, multiple sequence alignment, secondary and tertiary structure prediction to determine the biological function of genes. In addition, bioinformatics analysis was conducted to verify if they behave as other known invertebrate TLRs (Gong et al., 2017).

The protein sequence or primary structure decides the function and stability of the protein (Ghosh et al., 2019). Therefore, analyzing the amino acid sequence, which provides basic information about TLR6 and TLR13, was important. The isoelectric point (pI) reflected the solubility of a protein at a given pH (Han et al., 2018). The theoretical point (pI) of TLR6 and TLR13 was 5.47 and 5.9, respectively which suggests that the protein is acidic in nature. Twelve and thirteen N-glycosylation sites were predicted in TLR6 and TLR13, respectively. TLRs contain several N-linked glycosylation sites that may influence the surface pattern recognition of the receptor (Mekata et al., 2008; Srisuk et al., 2014; Yang et al., 2008). Although potential N-linked glycosylation sites were identified in the TLR6 and TLR13, the strict positions of important residues in the concave surface of LRRs have not been determined.

TLR6 and TLR13 exhibited typical TLR structures, including a single peptide, an extracellular LRR region, a transmembrane domain and an intracellular TIR domain. The structures were similar to domain structures of other crustaceans (mud crab), (giant tiger shrimp), and teleost fish (orange-spotted grouper) (Arts et al., 2007; Lin et al., 2012; Wang et al., 2016). In addition, TLR6 and TLR13 were compared with other known TLR vertebrates. However, both TLR6 and TLR13 possessed different numbers and distribution patterns

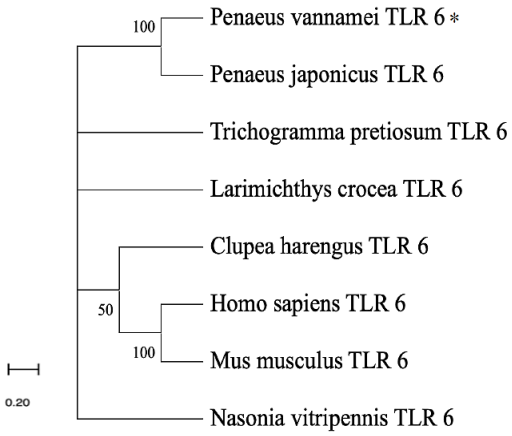

Figure 4. Phylogenetic tree analysis of the deduced amino acid sequences of TLR6 with different organisms using neighbor-joining method.

of LRR domains with their counterparts. Several studies reported the LRR domain as essential for pathogen recognition and ligand binding, which differ in number and position (Bell et al., 2003; Wan et al., 2022). The number of LRRs varying may suggest that TLR6 and TLR13 may recognize distinct ligands due to LRR variation and identify different pathogens (Arts et al., 2007; Gao et al., 2016; Han et al., 2018; Nie et al., 2018).

Further, multiple sequence alignment of amino acids of TLR6 with *Homo sapiens* (Human) and *Mus musculus* (Mouse) showed one conserved region in the LRR domain indicating that it might recognize a similar ligand as mammalian TLR6(Liang et al., 2018). Multiple sequence alignment of amino acids of TLR13 with *Miichthys miiuy* (Miu), *Rattus norvegicus* (Brown rat), and *Epinephelus coloides* (Orange-spotted grouper) showed three conserved regions in the LRR domain indicating TLR13 might recognize similar ligand as fish and mammalian TLR13 (Liang et al., 2018).

The phylogenetic analysis showed 100% similarity with *Penaeus japonicus* in TLR6 and 72% similarity with *Penaeus monodon* indicating it might be derived from a common ancestral gene. The relationship within the clusters indicates the taxonomic location of these species in evolution, with a possible function in the immune response (Gong et al., 2017). It was proposed that the LRRs may form a horseshoe-shaped structure with the ligand binding to the concave surface (Lin et al., 2012; Yang et al., 2007). TLR6 and TLR13 also possess a horseshoe-shaped arrangement LRR domain, indicating their potential capability to recognize PAMPs.

Tissue Distribution of TLR6 and TLR13

The tissue distribution of TLR6 and TLR13 in healthy tissues was investigated using qPCR. Both TLR6 and TLR13 exhibited ubiquitous expression, indicating their presence in all tested tissues, suggesting the possibility of reacting upon an invasion of a pathogen (Arts et al., 2007; Mekata et al., 2008). However, their expression levels varied among different tissues, suggesting potential tissue-specific functions. TLR6 was highly expressed in total hemocytes and the heart, while TLR13 was highly expressed in the intestine. Hemocyte and intestine are key immune or mucosal immune tissues, responsible for the defense against pathogens (Habib et al., 2021; Liang et al., 2018). Furthermore, the tissue expression of TLR13 was different in various species. For instance, *Epinephelus coioides* (Orange-spotted grouper) TLR13, the highest expression was observed in the brain (Liang et al., 2018). Similarly, in *Perciformes, Sciaenidae* (Miiuy croaker) the highest level was observed in the liver, spleen and kidney (Wang et al., 2016). These studies suggest that genes may be species-specific for the expression. In addition, the result suggested the maximum level of expression in immune-related tissue. These findings could imply the potential role of TLR6 and TLR13 in shrimp innate immunity.

Expression of TLR6 and TLR13 Following *V. harvyei* Infection

Gill and hepatopancreas were selected to analyze relative expression after the *Vibrio harveyi* infection. They are two crucial immune tissues in crustaceans. These tissues have been shown to be involved in shrimp immunity, protecting the shrimp from pathogens with higher TLR expression levels (Habib et al., 2021; Wan et al., 2022). TLR6 expression inducing at 24h suggests an early activation of the immune response. Meanwhile, TLR6 showed another significant up-regulation at 72h. This suggests that the best protection time was during 72h when it is challenged with *Vibrio harveyi* (Dechamma et al., 2015). These results are consistent with several studies that reported up-regulation in crustaceans during bacterial challenge (Lin et al., 2012; Wang et al., 2012; Yang et al., 2008). The upregulation also suggests that TLR6 has a potential role in *Litopenaeus vannamei* for bacteria, *Vibrio harveyi*.

TLR13 expression in the gills showed variable expression patterns throughout the time course of

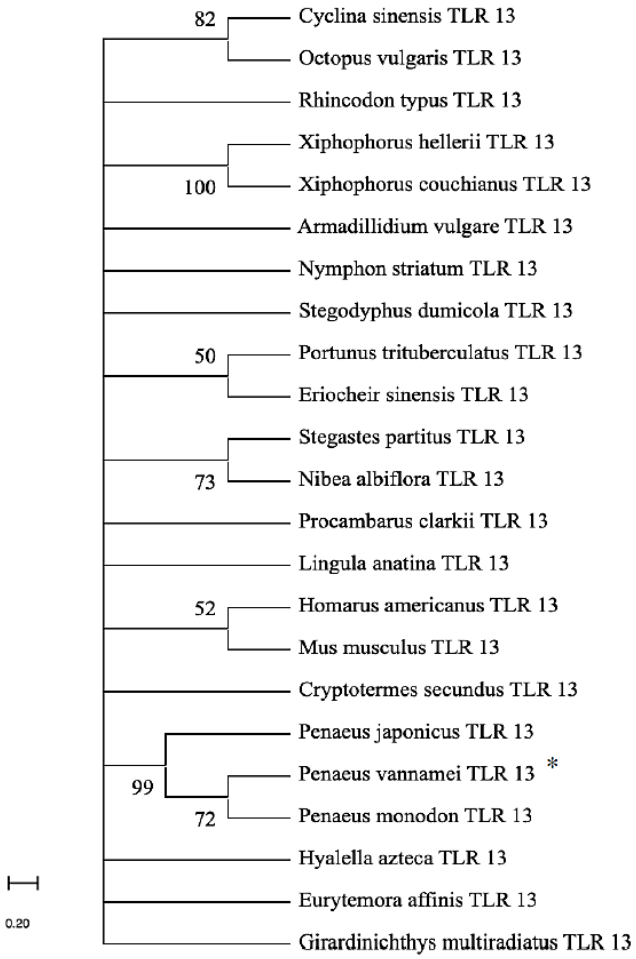

Figure 5. Phylogenetic tree analysis of the deduced amino acid sequences of TLR13 with different organisms using neighbor-joining method.

infection. TLR13 was induced at 24h suggesting early immune response. However, the expressions of TLR13 declined at 48h, followed by no difference at 72h. The result suggests that TLR13 may not play a prominent role in the early immune response during *V. harveyii* infection but could potentially be involved in the later stages of the immune response. Furthermore, the relative expression levels of TLR13 in the hepatopancreas were examined in response to *Vibrio harveyi* challenge. However, TLR13 expression didn't show any significant difference in hepatopancreas. In contrast to this study, TLR13 in whiteleg shrimp showed upregulation upon infection with Vibrio parahaemolyticus (Habib et al., 2021). The result obtained from this study suggests that TLR13 might not be directly involved in immune function against *V. harveyi* pathogen.

Conclusions

In conclusion, two TLRs (TLR6 and TLR13) were identified from *Litopenaeus vannamei* (Whiteleg shrimp), and subsequently characterized using bioinformatics tools. The TLR6 and TLR13 were expressed in all tested healthy tissues. However, different expression patterns were observed in the study by qPCR. After a bacterial challenge, the expression of TLR6 in the gills was significantly regulated. Meanwhile, the expression of TLR13 was observed in the gills while hepatopancreas didn't show any significant differences. Overall, TLR6 and TLR13 suggest they may play a role in the immune response against the pathogen. The results obtained in this study serve as a basis for understanding the shrimp and pathogen interaction during infection and disease outbreaks. However, a future study must be carried out to understand the specific ligands recognized by Whiteleg TLR6 and TLR13, as well as their downstream signalling pathways. This can provide a deeper understanding of the immune mechanisms involved in shrimp-pathogen interactions.

Ethical Statement

No human subjects were included in this study. At the moment there is no permission required from the National Pingtung University of Science and Technology Experimental Animal Ethics Committee, to conduct studies on shrimp.

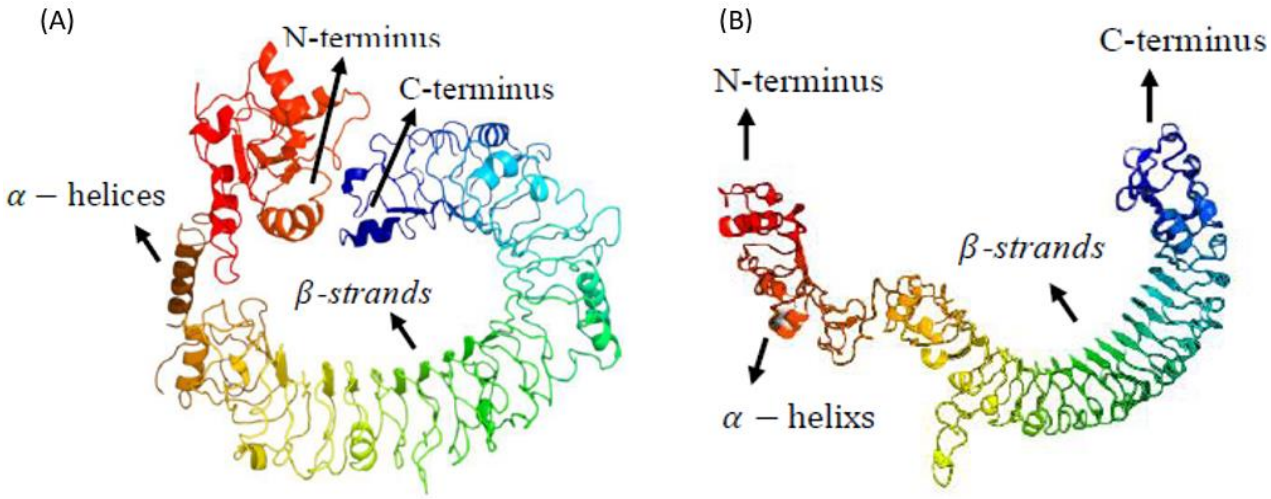

Figure 6. Schematic representation of predicted protein 3D model of *Litopenaeus vannamei* (Whiteleg shrimp) TLR6 and TLR13 using Phyre2.

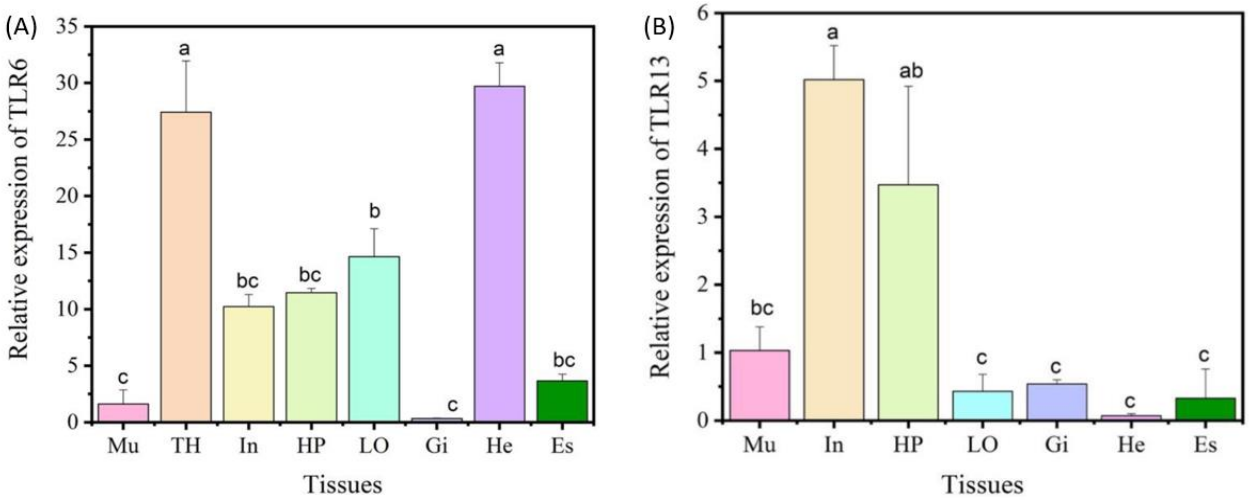

Figure 7. Relative expression of TLR6 (A) and TLR13 (B) in different tissues of *Litopenaeus vannamei*, quantified by qPCR. The relative gene expression levels were normalized with *β-actin*. Different lowercase letters (abc) meant significant difference (P<*0.05*) among tissues. Values are shown as the means ± standard deviation (n=3). Abbreviations used: Total hemocytes-TH; Intestine- In; Hepatopancrease-HP; Lymphoid organ-LO; Gill-Gi; Heart-He; Muscle-Mu; Eyestalk-Es.

Funding Information

This work did not receive any funding support.

Author Contribution

All authors contributed to the study conception and design. Conceptualization, methodology, writing - review and editing, and validation were performed by Sunita Subedi. Sudarshan Pandey contributed to data analysis and methodology. Supervision, and writing - review and editing were performed by Omkar Vijay Byadgi. The first draft of the manuscript was written by Sunita Subedi and all authors commented on previous versions of the manuscript. All authors read and approved the final manuscript**.**

Conflict of Interest

The authors declare that they have no known competing financial or non-financial, professional, or personal conflicts that could have appeared to influence the work reported in this paper.

Acknowledgements

The first author is grateful for the National Pingtung University of Science and Technology's Scholarship for pursuing the master's degree. We thank Dr. Wahyu Purbiantoro for his assistance and discussion during the study.

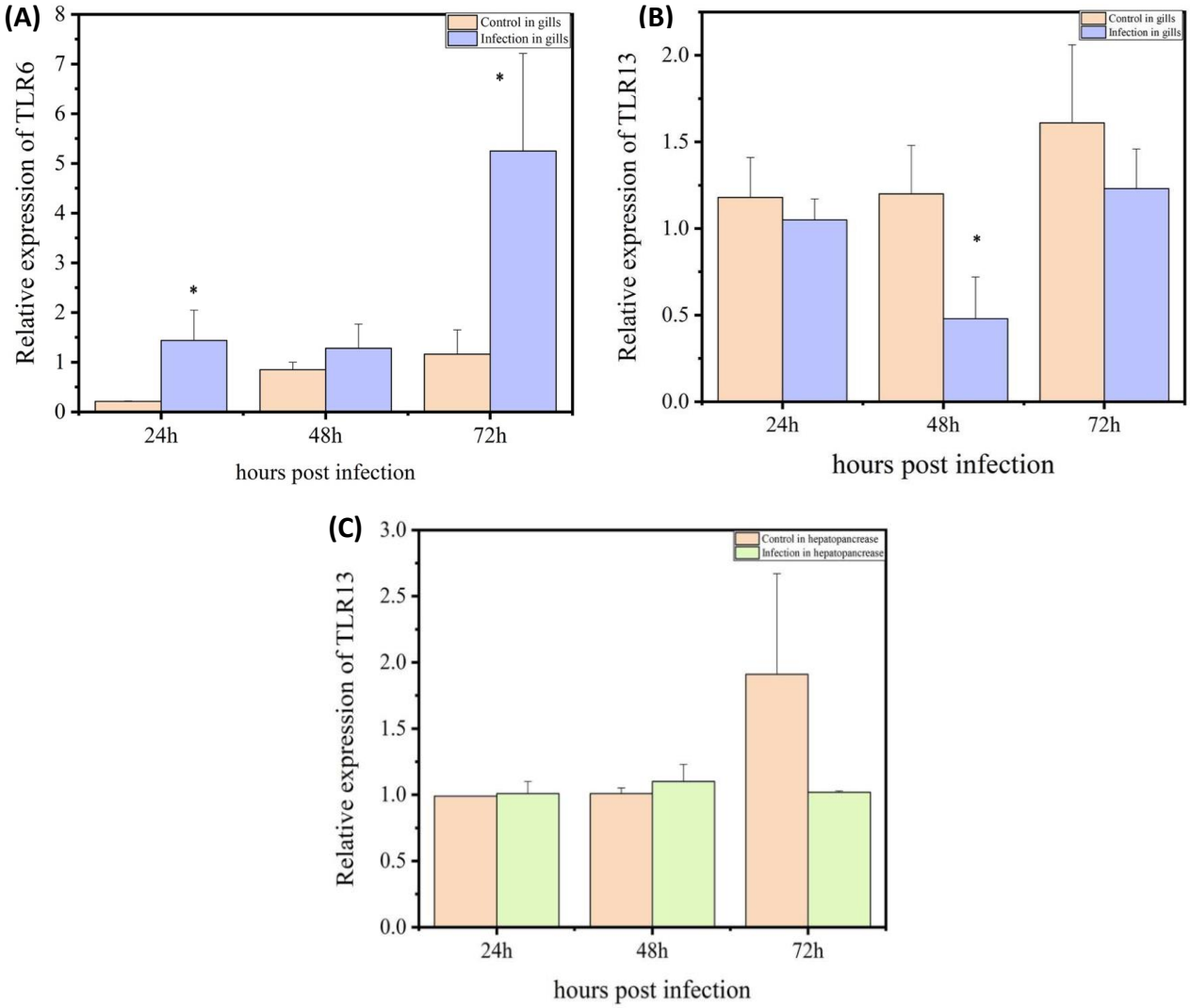

Figure 8. Relative expression of TLR6 in the gill (A) and TLR13 in the gill (B) and hepatopancrease (C) in response to *Vibrio harveyi*, quantified by q-PCR. The relative gene expression levels were normalized with β-actin. Y-axis indicates the relative expression level of respective TLR genes, normalized with the *β-actin* gene while Xaxis indicates hours post bacterial infection at 24h, 48h, and 72 h, respectively. The significant difference between the challenged and PBS control group is denoted with * at P<0.05.

References

Anderson KV, Bokla L, Nüsslein-Volhard C (1985) Establishment of dorsal-ventral polarity in the drosophila embryo: the induction of polarity by the Toll gene product. *Cell*. https://doi.org/10.1016/0092-8674(85)90275-2

Artimo P, Jonnalagedda M, Arnold K et al., (2012) ExPASy: SIB bioinformatics resource portal. *Nucleic Acids Research*. https://doi:10.1093/nar/gks400

Arts JAJ, Cornelissen FHJ, Cijsouw T et al., (2007) Molecular cloning and expression of a Toll receptor in the giant tiger shrimp, *Penaeus monodon*. *Fish and Shellfish Immunology*. https://doi.org/10.1016/j.fsi.2006.08.018

Asche F, Anderson JL, Botta R et al., (2021) The economics of shrimp disease. *Journal of Invertebrate Pathology*. https://doi.org/10.1016/j.jip.2020.107397

Bell JK, Mullen GED, Leifer CA et al., (2003) Leucine-rich repeats and pathogen recognition in Toll-like receptors. *Trends in Immunology*. https://doi.org/10.1016/S1471-4906(03)00242-4

Madeira, F, Pearce, M, Tivey, ARN, et al., (2022). Search and sequence analysis tools services from EMBL-EBI in 2022. *Nucleic Acids Research*, 50(W1), W276–W279. https://doi.org/10.1093/nar/gkac240

Dechamma MM, Rajeish M, Maiti B et al., (2015) Expression of Toll-like receptors (TLR), in lymphoid organ of black tiger shrimp (*Penaeus monodon*) in response to *Vibrio harveyi* infection. *Aquaculture Reports*. https://doi.org/10.1016/j.aqrep.2015.02.002

ExPASy (2022) Retrieved 17 September, 2022, from http://web.expasy.org/protparam

FAO (2020) Food and Agriculture Organization of the United Nations, Fishery and Aquaculture Statistics. http://www.fao.org/fishery/statistics/software/fishstatj

Gao Q, Xiao Y, Zhang C et al (2016) Molecular characterization and expression analysis of toll-like receptor 2 in response to bacteria in silvery pomfret intestinal epithelial cells. *Fish and Shellfish Immunology*. https://doi.org/10.1016/j.fsi.2016.08.057

Ghosh R, Upadhyay A, Roy A, Tiwari A (2019) Structural and functional analysis of aquaporin protein of different fish

species. *Journal of Entomology and Zoology Studies* 7(5):94-107

Gong Y, Feng S, Li S, Zhang Y et al., (2017) Genome-wide characterization of Toll-like receptor gene family in common carp (*Cyprinus carpio*) and their involvement in host immune response to *Aeromonas hydrophila* infection. *Comparative Biochemistry and Physiology Part D: Genomics and Proteomics*. https://doi.org/10.1016/j.cbd.2017.08.003

Gupta, R, & Brunak, S (2002). Prediction of glycosylation across the human proteome and the correlation to protein function. Pacific Symposium on Biocomputing. Pacific Symposium on Biocomputing, 310–322.

Habib YJ, Wan H, Sun Y, Shi J et al., (2021) Genome-wide identification of toll-like receptors in Pacific white shrimp (*Litopenaeus vannamei*) and expression analysis in response to *Vibrio parahaemolyticus* invasion. *Aquaculture*. https://doi.org/10.1016/j.aquaculture.2020.735996

Habib YJ, and Zhang Z (2020) The involvement of crustaceans toll-like receptors in pathogen recognition. *Fish and Shellfish Immunology*. https://doi.org/10.1016/j.fsi.2020.04.035

Han P, Wang S, Zhang Q, Zhang S et al., (2018) Molecular characterization and expression analysis of TLR1 and TLR4 from the endangered fish Dabry's sturgeon (*Acipenser dabryanus*). *Developmental and Comparative Immunology*. https://doi.org/10.1016/j.dci.2018.05.009

Huang Y, and Ren Q (2020) Research progress in innate immunity of freshwater crustaceans. *Developmental and Comparative Immunology*. https://doi.org/10.1016/j.dci.2019.103569

Jiao L, Dai T, Zhong S, Jin M, Sun P, Zhou Q (2021) *Vibrio parahaemolyticus* infection influenced trace element homeostasis, impaired antioxidant function, and induced inflammation response in *Litopenaeus vannamei*. *Biological Trace Element Research*. https://doi.org/10.1007/s12011-020-02120-z

Letunic I, Copley RR, Pils B, Pinkert S, Schultz J, Bork P (2006) SMART 5: domains in the context of genomes and networks. *Nucleic Acids Research*. https://doi.org/10.1093/nar/gkj079

Liang Y, Ding X, Yu X, Wang Y, Zhou Y et al., (2018) Identification and functional characterization of Toll-like receptor 13 from orange-spotted grouper (*Epinephelus coioides*). *Fish and Shellfish Immunology.* https://doi.org/10.1016/j.fsi.2017.12.054

Lin Z, Qiao J, Zhang Y, Guo L et al., (2012) Cloning and characterisation of the SpToll gene from green mud crab, *Scylla paramamosain*. *Developmental and Comparative Immunology.* https://doi.org/10.1016/j.dci.2011.09.003

Livak K J and Schmittgen TD (2001) Analysis of relative gene expression data using real-time quantitative PCR and the $2^{-\Delta\Delta CT}$ method. *Methods*. https://doi.org/10.1006/meth.2001.1262

McGuffin LJ, Bryson K, Jones, DT (2000) The PSIPRED protein structure prediction server. *Bioinformatics*. https://doi.org/10.1093/bioinformatics/16.4.404

MEGA. (2022). Retrieved November 12, 2022 from https://www.megasoftware.net/

Mekata T, Kono T, Yoshida T, Sakai M, Itami T (2008) Identification of cDNA encoding Toll receptor, MjToll gene from kuruma shrimp, *Marsupenaeus japonicus*. *Fish and Shellfish Immunology*. https://doi.org/10.1016/j.fsi.2007.10.006

NCBI Genome Database 2022 Retrieved September 7, 2022, from http://www.ncbi.nlm.nih.gov/

NetNGlyc (2022) Retrieved November 18, 2022, from https://services.healthtech.dtu.dk/services/NetNGlyc-1.0/

Nie L, Cai S-Y, Shao J-Z, Chen J (2018) Toll-like receptors, associated biological roles, and signaling networks in non-mammals. *Frontiers in Immunology.* Retrieved from https://www.frontiersin.org/journals/immunology/articles/10.3389/fimmu.2018.01523

Niu S, Zhu Y, Geng R, Chen N, et al., (2023) A novel Toll receptor from Pacific white shrimp *Penaeus vannamei* is involved in immune defense against *Vibrio parahaemolyticus* infection. *Aquaculture*. https://doi.org/10.1016/j.aquaculture.2023.739396

Phyre2 (2022) Retrieved November 10, 2022, from http://www.sbg.bio.ic.ac.uk/~phyre2/html/page.cgi?id=index

PSIPRED (2022) Retrieved November 5, 2022, from http://bioinf.cs.ucl.ac.uk/psipred/psiform.html

Purbiantoro W, Huynh-Phuoc V, Castillo-Corea B R J, Byadgi OV, Cheng TC (2024) Effectiveness of dietary heat-killed *Bacillus subtilis* harboring plasmid containing 60 copies of CpG-ODN 1668 against *Vibrio harveyi* in *Penaeus vannamei*. *Veterinary Research Communications*. https://doi.org/10.1007/s11259-023-10182-2

Qin Z, Babu VS, Wan Q, Zhou M et al (2018) Transcriptome analysis of Pacific white shrimp (*Litopenaeus vannamei*) challenged by *Vibrio parahaemolyticus* reveals unique immune-related genes. *Fish and Shellfish Immunology*. https://doi.org/10.1016/j.fsi.2018.03.030

Sánchez-Salgado JL, Pereyra MA, Alpuche-Osorno JJ, Zenteno E (2021) Pattern recognition receptors in the crustacean immune response against bacterial infections. *Aquaculture*. https://doi.org/10.1016/j.aquaculture.2020.735998

SMART (2022) Retrieved September 9, 2022, from http://smart.embl-heidelberg.de/

Srisuk C, Longyant S, Senapin S, Sithigorngul P, Chaivisuthangkura P (2014) Molecular cloning and characterization of a Toll receptor gene from *Macrobrachium rosenbergii*. *Fish and Shellfish Immunology*. https://doi.org/10.1016/j.fsi.2013.12.025

Tamura K, Stecher G, Kumar S (2021) MEGA11: Molecular Evolutionary Genetics Analysis Version 11. *Molecular Biology and Evolution*. https://doi.org/10.1093/molbev/msab120

Wan H, Mu S, Baohua D, Guo S, Kang X (2022) Genome-wide investigation of toll-like receptor genes (TLRs) in Procambarus clarkia and their expression pattern in response to black may disease. *Fish and Shellfish Immunology*. https://doi.org/10.1016/j.fsi.2022.10.066

Wang PH, Liang JP, Gu ZH, Wan DH, Weng SP, Yu XQ, He JG (2012) Molecular cloning, characterization and expression analysis of two novel Tolls (LvToll2 and LvToll3) and three putative Spätzle-like Toll ligands (LvSpz1–3) from *Litopenaeus vannamei*. *Developmental and Comparative Immunology*. https://doi.org/10.1016/j.dci.2011.07.007

Wang XW, Wang JX (2013) Pattern recognition receptors acting in innate immune system of shrimp against pathogen infections. *Fish and Shellfish Immunology*. https://doi.org/10.1016/j.fsi.2012.08.008

Wang Y, Bi X, Chu Q, Xu T (2016) Discovery of toll-like receptor 13 exists in the teleost fish: Miiuy croaker (*Perciformes, Sciaenidae*). *Developmental and Comparative*

Immunology. https://doi.org/10.1016/j.dci.2016.03.005

Yang C, Zhang J, Li F, Ma H et al., (2008) A Toll receptor from Chinese shrimp *Fenneropenaeus chinensis* is responsive to *Vibrio anguillarum* infection. *Fish and Shellfish Immunology*. https://doi.org/10.1016/j.fsi.2007.12.012

Yang LS, Yin ZX, Liao JX, Huang XD et al., (2007) A Toll receptor in shrimp. *Molecular Immunology*. https://doi.org/10.1016/j.molimm.2006.09.021

Yu YB, Choi JH, Kang JC, Kim HJ, Kim JH (2022) Shrimp bacterial and parasitic disease listed in the OIE: A review. *Microbial Pathogenesis*. https://doi.org/10.1016/j.micpath.2022.105545

Zhou SM, Yuan XM, Liu S, Li M, Tao Z, Wang GL (2015) Three novel Toll genes (PtToll1–3) identified from a marine crab, *Portunus trituberculatus*: Different tissue expression and response to pathogens. *Fish and Shellfish Immunology*. https://doi.org/10.1016/j.fsi.2015.07.027

(A)

```
Name:  Sequence          Length:  1349
MKNTVALYVFASVFASCSVAFVYNAPENCDWTFRDEAQREVSLSCSLRTIGNDFDSSNFSIAQSEHTTELEILCSDVLFF      80
QSSLQPRVFQRLYNLDTISIEFCKLTSLPAGAFLGLDAMKALAVRTHNSDWSAMALELNPDSLVGMPHLERLDLGQNNIW     160
NLPERVFCPLPALRHLNLTWNRLQDVSEVGVSGSCGAHLVTLDLSGNDLVVLPEAGLAGLESLRELYLQYNDVSMLADGA     240
FSGLSTLSVLNISSNRLVALPPEVFNETLGLTELHLQNNSLSVLAPGLFSALSRLTVLDMSFNQLTSEWVTAETFRGLLR     320
LVVLNLSHNRLTQVTLDMFRDLSTLQVLDLRHNSLTVLGDMTFSPLANLHRLDLSYNSLVSVESRGLSGLHVLASLSVAH     400
NNISRIAPEAFQNCTSLRDLRLEYNLLEEIPEAVREASSLRTLRISHNQLSAVAQGDLTSLSALRHLDMSNNFLRGLCKS     480
CLAGLEYLEVLDLSQNELSTVPHGAFDTNTGLQLLRMDGNKMSDINGLFASLSNLLWLNVSDNRISWFDYALIPDQLQYL     560
DLHNNRIRDLGNYFSLESKLELRTLDVSHNQLESLSASSVPDSVELLFVNSNKITRIATGTFAEKRNLSMVDLYDNLLSK     640
IDLNSINLPRVPEERDLPEFYIGGNPIFCDCNMEWMHRVHQISSLRQHPRVMDLDKVTCTLPYPRSAENRVPFLETQPSQ     720
FLCPYTSHCFALCHCCDFIACDCQMTCPIGCSCYHDGTWATNIVDCSARNHHQLPDDIPMDATLVYMDGNEMPFLDAHHL     800
IGRKNMRALYLNSSRVERIQNRTFHGLSTLKELHLHDNMLVELEGFEFEHLEHLRELYLQNNRLKVINNVTFAGLKSLEV     880
LRLDGNFLFEFPVWHLKLNKGLKDVTLGINLWSCECQYMVDFKNWLIRETDVVKDAKSIFCVSNSTGEPGPYVLESSYSC     960
ENFVATSIVQEKLENDFLQPVLITLAIFFVVLVMGVVFAVFRVRLQASVSKKCGLKCFPSQPAPAKEEERNMLYDAFVSY    1040
SEMDAPFVTEVFAAELENGDPSYKVCLSSRDYQTVGSYVGDFIVQSIETSHKVVLVLTKNFVDHDWCKFSFKAAHVEALK    1120
SLKNRVIVVMCGDVDESDMDSDLSGIVKSATKLKYEDKSFWSKLHAALPGGAKKMSQQCYITETNYIMRNSVPVLSPNHN    1200
LKQSQFMPNMVLTNTLKTPVSHYHQQHHYQHTQPSINSDTGDLDKTFVSVETAQSSLAPSLNHSYMSIDYAAARNSHIYA    1280
SIDETTPALPPSTLPSVHTLHQHLRQQQHVEPLRQYLPQDVLSSQQRRPLTGAPMQTFDQPAVSASYFI
```

(B)

```
Name:  Sequence          Length:  1092
MLVSRLTALVFGLLVVLVSLSLGAAIRGASGFPHSSLRRVKSPVSQNDFLGPSDSKGSDERHGEATVGEVPRTLDLSLNV      80
KVTENGRYDNDAVSYVSQAGGNGYAAEKRATEELVKNGERLTSSAMTDEVLTTKTKTQERKEASKNQVPFLSSTKSFQKS     160
EESALVSEDPTFPSTGKGRIKEEKGDTAKNETRSSHAKNRCEFRSAPPDVVFPDAFEEFSRSMEANLSPDDQPDEELLDS     240
LLPDGCHYTERQKKKVMCTGANMTSIPEFEHARNIETLHFSGTSIVQVTNLDPLPRSLKALYFSNGMLKVFDGRNLNRVS     320
GLEVLHLDNNFITSWSLVTTFYSMGGFAEQNTIKTLNIRSNQITYPPQPVGDNETVLPYLETFVLSENPLCYLPDTLFKP     400
LRNSNVTSLYLKNCNIDEFYGSPLSYLPNLEVLDLTGNRAINETELRDLLLPLGRLKQLFLGNNNYQTVPTKALSLVNGT     480
LENLDLHSSTFTCLDNSSFPIMPVLTHLDLKYCRINAIREHTFQGFPMLRELNLDGNSLTTVPPEVLLPSLQILTLSDNP     560
RANGNDGDQRFSMEDVSFQDMVNLKTIQLNQVIMEKIERSYFNDLYNLEELSLTGCGIKTIENFSFVNLTKLQHLNLSEN     640
YITTLYNDSLVGLVNLISLDLSNNKLKGINRMGRSGVSSSAVRTDSLSSGTVSDAREIDSFLERVRAPSPLIPWLSSIRR     720
NARAVGPLGWQGKDLPRTTIAAYAFSDLVRLRTLNLSENMIMLLPPELFHNLTNLLILDISYNRLMTWDDPVLGSIPNLT     800
ELHLRTNLLDGITDAMEVDFRKESLKLVDLQDNTFKCDCSLSKFNRSLNTSHFLNWPYLCREGKADVDMEEYIARAPCNF     880
ATQPENHGRMRAIVISTIVSSLLLVASVMVYRKRWYVRYFMYTVRMRTKVVREEADKYLYDTFVCYSQTDRQWVFEHLVA     960
KLEDGGRYRVCIHERDFTVGQEITDNIINSVERSRKVVVVLSPAFIRSSWCMFELQMASNKILDERKSKLIMLLLEHIPD    1040
EEQPKKLKYLLKTRTYIEWVPDLESQKLFWARLMRAISKPSDSEAIAASTKL
```

Supplementary Figure 1. Predicted N-glycosylation sites of TLR6 (A) and TLR13 (B) of *Litopenaeus vannamei* (Whiteleg shrimp).

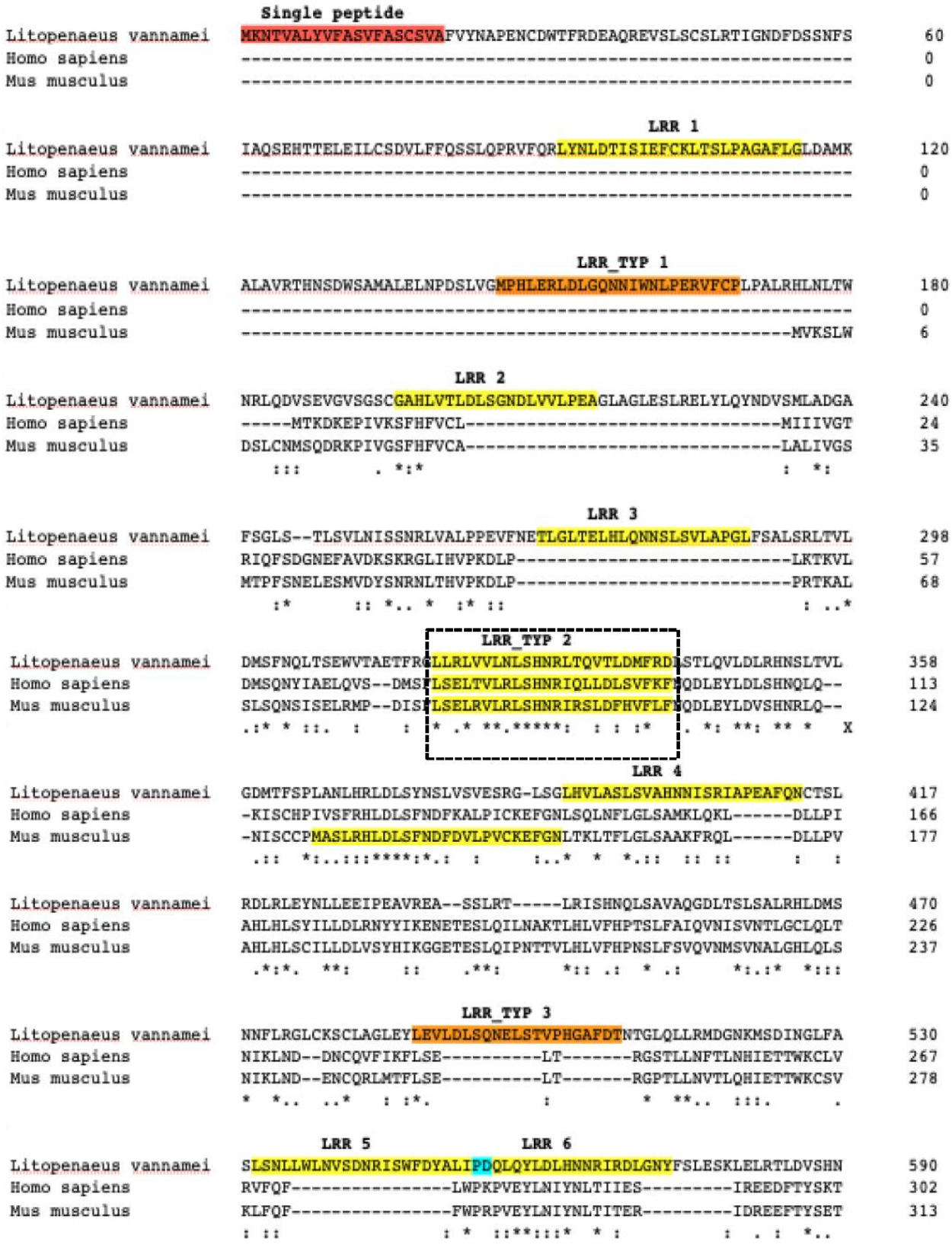
Single peptide
LRR 1
LRR_TYP 1
LRR 2
LRR 3
LRR_TYP 2
LRR 4
LRR_TYP 3
LRR 5
LRR 6
Litopenaeus vannamei
Homo sapiens
Mus musculus

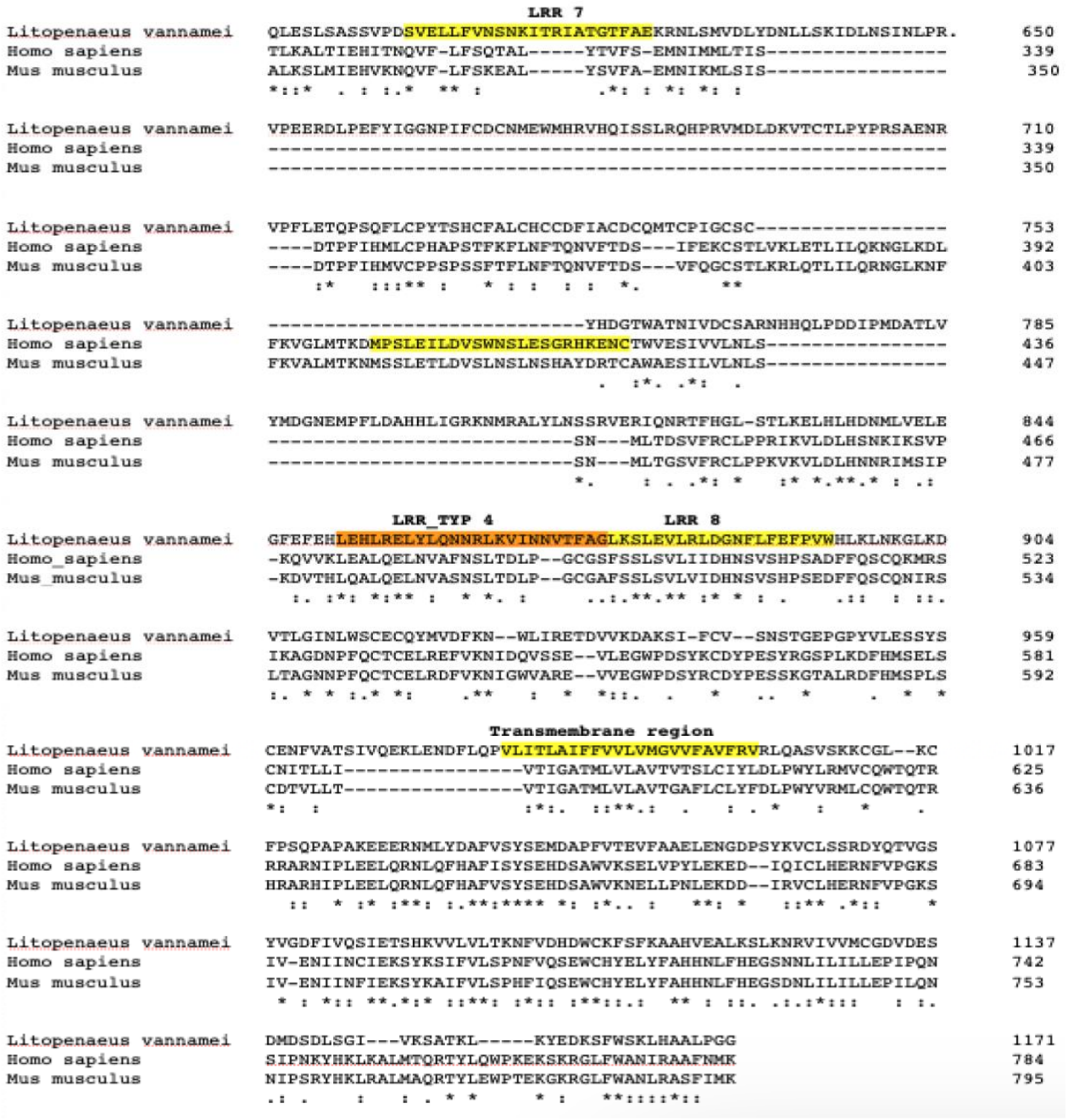

Supplementary Figure 2. Multiple sequence of *Litopenaeus vannamei* (Whiteleg shrimp) TLR6 with homologous sequences from other species. Conserved region indicated by highlights; - - -Sequence gaps, "*" identical residues, ":" conserved substitution, and "."semi conserved substitution. The single peptide, LRR motifs, and transmembrane (TM) region are indicated by colors. Single peptide: Red; LRR motifs: Yellow; LRR_TYP: Brown; Green: TR region; Overlapped: blue.

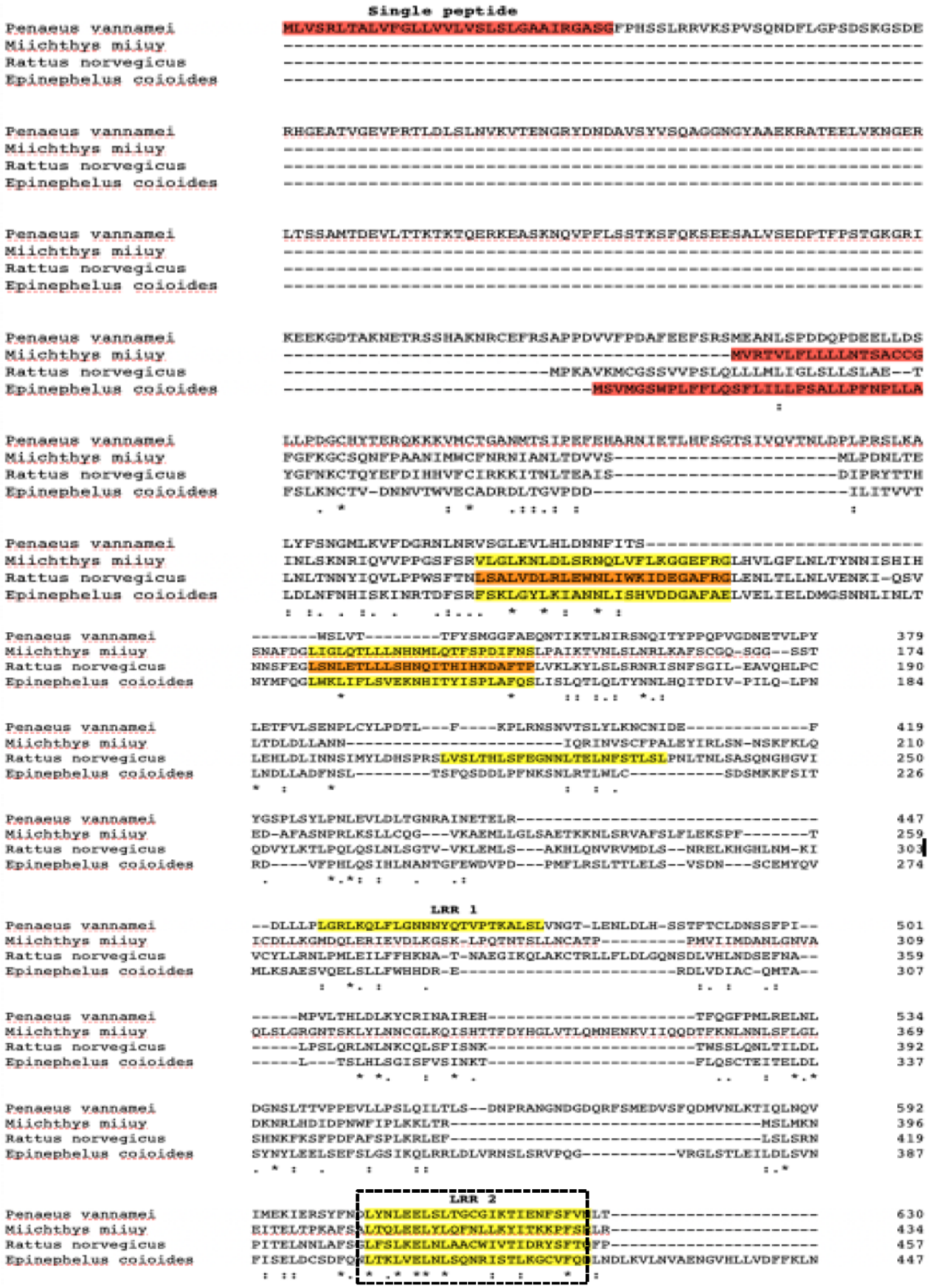
Single peptide
Penaeus vannamei
Miichthys miiuy
Rattus norvegicus
Epinephelus coioides
LRR 1
LRR 2

Supplementary Figure 3. Multiple sequence of *Litopenaeus vannamei* (Whiteleg shrimp) TLR13 with homologous sequences from other species. Conserved region indicated by highlights; - - -Sequence gaps, "*" identical residues, ":" conserved substitution, and "." semi conserved substitution. The single peptide,LRR motifs, and transmembrane (TM) region are indicated by colors. Single peptide: Red; LRR motifs: Yellow; LRR_TYP: Brown; Green: TR region.

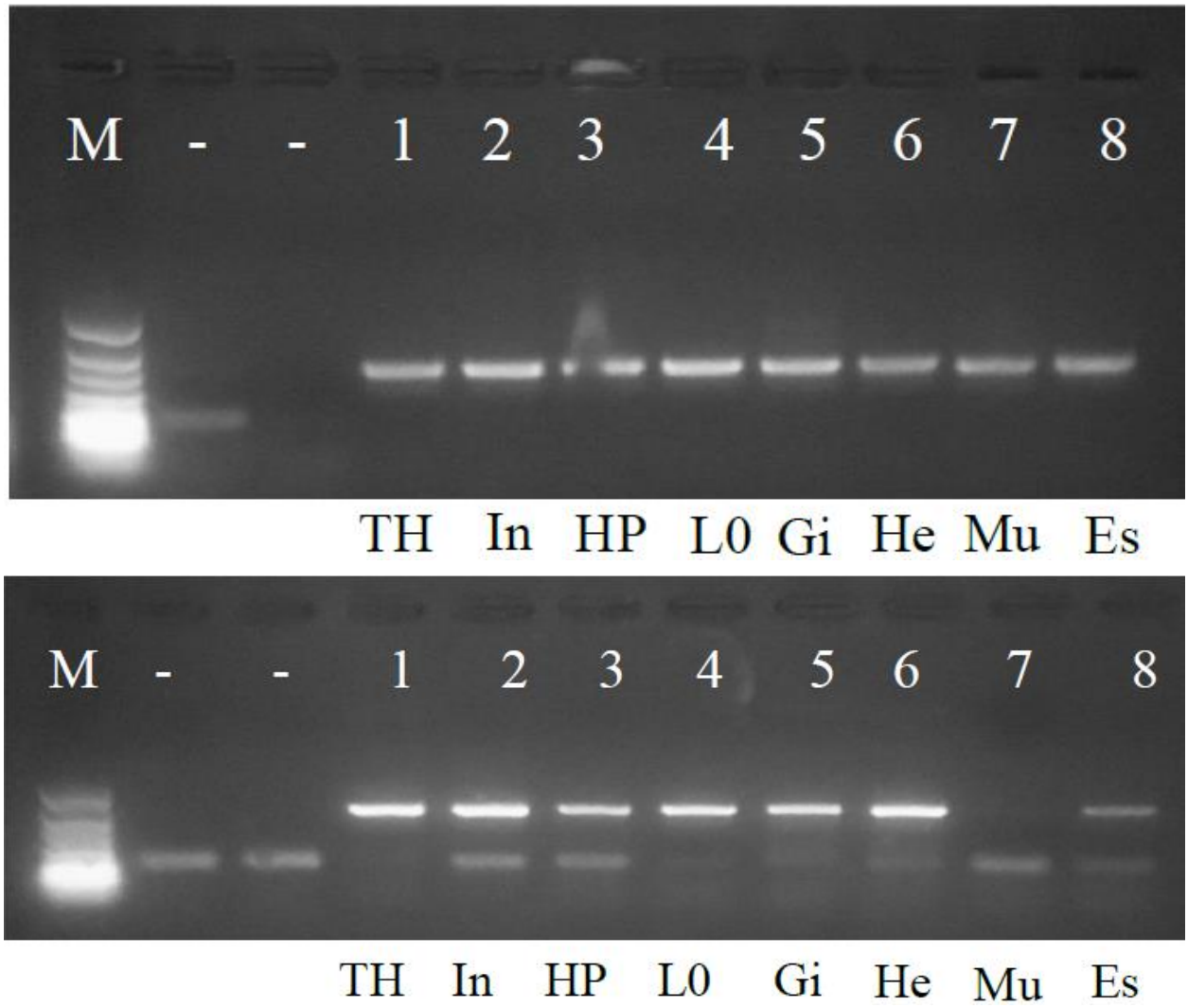

Supplementary Figure 4 Expression analysis of TLR6 in different tissues by PCR. *β-actin* gene was used as a control. Abbreviations used: 10 bp DNA marker (M), negative control (no cDNA); negative PCR (- no primer), negative RT-PCR (-), total hemocytes (TH) (lane 1), intestine (In) (lane 2), hepatopancrease (HP) (lane 3), lymphoid organ (LO) (lane 4), gill (Gi) (lane 5), heart (He) (lane 6), muscle (Mu) (lane 7), eye stalk (Es) (lane 8).

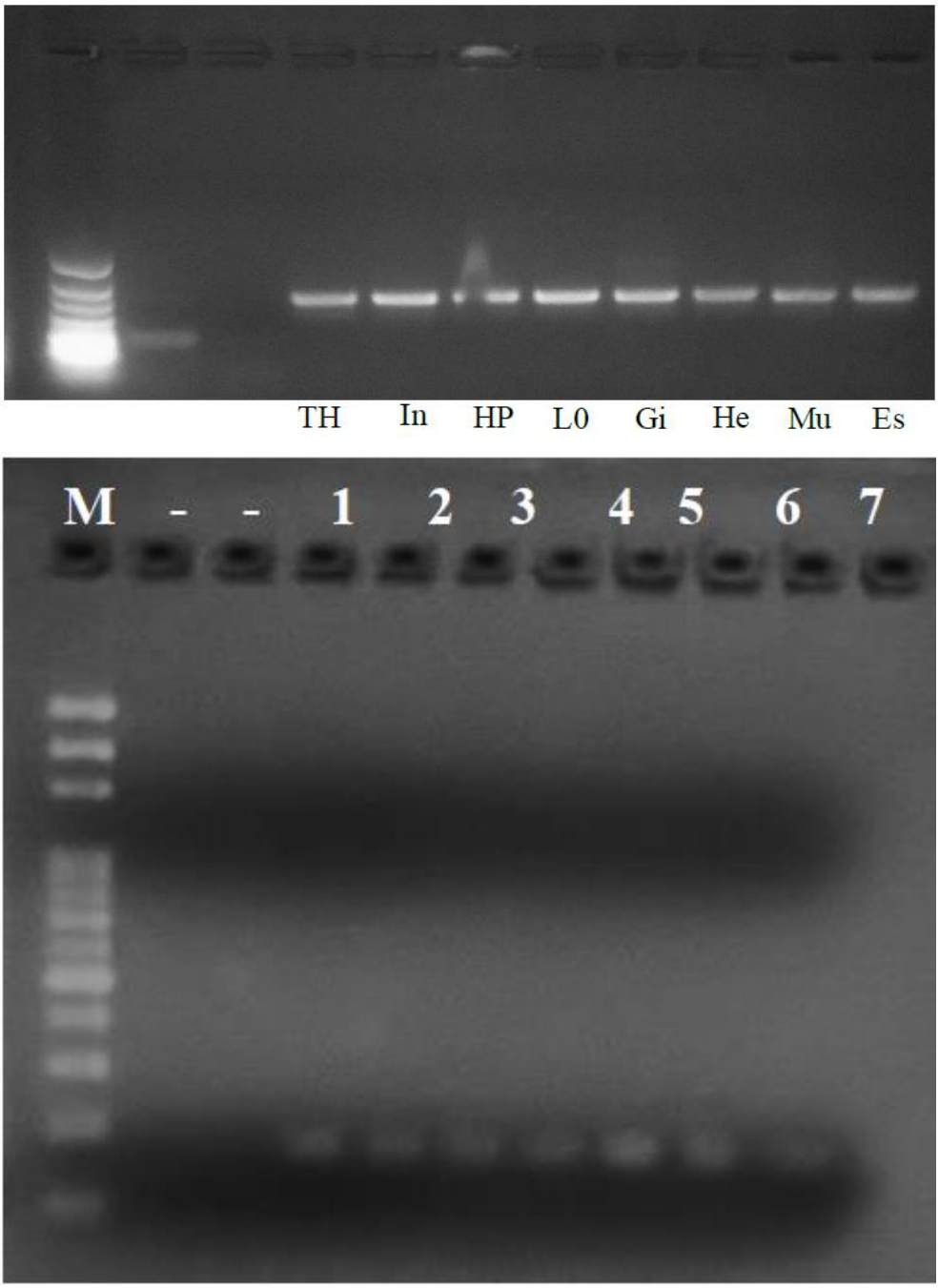

Supplementary Figure 5. Expression analysis of TLR13 in different tissues by PCR. *β-actin* gene was used as a control. Abbreviations used: 10 bp DNA marker (M), negative control; negative PCR (-no cDNA), negative control; negative RT-PCR (-no primer), total hemocytes (TH) (lane 1), intestine (In) (lane 2), hepatopancrease (HP) (lane 3), lymphoid organ (LO) (lane 4), gill (Gi) (lane 5), heart (He) (lane 6), muscle (Mu) (lane 7), eye stalk (Es) (lane 8).